

Hyaluronan and hyaluronan synthases expression and localization in embryonic mouse molars

Guofeng Yang¹ · Beizhan Jiang¹ · Wenping Cai² · Shangfeng Liu² · Shouliang Zhao^{1,2}

Received: 23 April 2016 / Accepted: 13 June 2016 / Published online: 18 June 2016
© Springer Science+Business Media Dordrecht 2016

Abstract Hyaluronan (HA) and hyaluronan synthases (HASs) have been shown to play critical roles in embryogenesis and organ development. However, there have not been any studies examining HA and HAS expression and localization during tooth development. The present study was designed to investigate the expression of HA and three isoforms of HASs (HAS1, 2, 3) in embryonic mouse molars. The first mandibular embryonic mouse molars were examined by immunohistochemistry at E11.5, E13.5, E14.5, E16.5, and E18.5. PCR and western blot analyses were performed on RNA and proteins samples from E13.5 to E18.5 tooth germs. At the initial stage (E11.5), HA and HASs were expressed in the dental epithelium but not the underlying dental mesenchyme. HA immunostaining gradually increased in the enamel organ from the bud stage (E13.5) to the late bell stage (E18.5), and HA and HASs were highly expressed in the stellate reticulum and stratum intermedium. HA immunostaining was also enhanced in the dental mesenchyme and its derived tissues, but it was not expressed in the ameloblast

and odontoblast regions. The three HAS isoforms had distinct expression patterns, and they were expressed in the dental mesenchyme and odontoblast at various levels. Furthermore, HAS1 and HAS2 expression decreased, while HAS3 expression increased from E13.5 to E18.5. These results suggested that HA synthesized by different HASs is involved in embryonic mouse molar morphogenesis and cytodifferentiation.

Keywords Hyaluronan · Hyaluronan synthase · Tooth germ · Tooth development · Mouse · Molar

Introduction

Tooth development depends on well-regulated reciprocal interactions between the dental epithelium and the dental mesenchyme (Xie et al. 2015; Lei et al. 2014). Through these continuous epithelial-mesenchymal interactions, the tooth primordium progresses from the dental lamina stage through the bud, cap and bell stages to the formation of tooth crown and roots (Thesleff 2003). The precise molecular mechanisms that mediate the interactions between the epithelium and mesenchyme have not been clearly elucidated. However, it is well accepted that stage-specific extracellular matrices (ECMs) play essential roles in epithelial-mesenchymal interactions (Bei 2009).

Hyaluronan (hyaluronic acid, HA) is a non-sulfated glycosaminoglycan composed of the repeating polymeric disaccharides *N*-acetylglucosamine (*GlcNAc*) and *glucuronic acid* (*GlcA*). It is a major extracellular matrix component (Vigetti et al. 2014) widely expressed in many tissues, including cartilage, skin, smooth muscle, and other connective tissues. By serving as a scaffold or by interacting with other matrix proteins or receptors, such as

Guofeng Yang and Beizhan Jiang these authors contributed equally to this work and should be considered as co-first authors.

✉ Beizhan Jiang
jiangbeizhan@tongji.edu.cn

✉ Shouliang Zhao
slzhao@fudan.edu.cn

¹ Department of Endodontics, School & Hospital of Stomatology, Tongji University, Shanghai Engineering Research Center of Tooth Restoration and Regeneration, Shanghai 200072, People's Republic of China

² Department of Stomatology, Huashan Hospital, Fudan University, Shanghai 200040, People's Republic of China

CD44, RHAMM and versican, the hyaluronan-dependent pericellular matrix can directly or indirectly function in the assembly of other ECM components (Evanko et al. 2007) and consequently plays multiple roles in several physiological and pathological conditions (Jiang et al. 2011), including embryogenesis and organ development (Itano 2008).

HA is biosynthesized by three membrane-bound hyaluronan synthases (HAS1, 2, 3) (Weigel et al. 1997). Until now, the multiple functions of the HASs were unclear (Siiskonen et al. 2015; Tian et al. 2013; Wang et al. 2015). However, it is clear that their functions are highly dependent on the size of HA that they each produce (Stern et al. 2006). HAS1 and HAS2 synthesize the high-molecular weight HA (HMW HA), and HAS3 synthesizes the low-molecular weight HA (LMW HA) (Itano and Kimata 2002). In addition, LMW HA has been reported to increase cell proliferation and cell differentiation, while HMW HA facilitates cell contact inhibition, though this has been debated. HAS2 is expressed throughout all stages of embryonic development, and loss of the gene is embryonic lethal (Camenisch et al. 2000). HAS1 is prominently expressed in the early stages of midblastula, gastrulation and neurulation, while HAS3 is expressed later in development when sensory organs begin to form (Tien and Spicer 2005).

The expression and distribution of HA and HASs in tooth development has been partially described previously. Previous studies have reported the localization of HA in the postnatal rat molar dental pulp (Shibata et al. 1999, 2002) and human tooth germs at the cap stage and bell stage. Tien et al. performed *in situ* hybridization to detect HAS distribution in early mouse embryonic tooth molars (Tien and Spicer 2005), and Felszeghy performed immunohistochemistry in the bell stage of human tooth germs (Felszeghy et al. 2005). Unfortunately, these studies did not comprehensively cover all of the stages of tooth development, nor did they examine HAS expression levels. Therefore, we performed this study to compare the developmental changes and regional differences of HA and HAS expression at various stages of the development of the first mandibular embryonic mouse molars.

Materials and methods

Animals

Pregnant institute of Cancer Research (ICR) mice were ordered from Slaccas (Shanghai, China), and maintained under standard conditions at the Animal Center of the Stomatology Hospital of Tongji University. The animal-use protocol conformed to the National Institutes of Health guidebook and was reviewed and approved by the

Screening Committee for Animal Research of Tongji University. The presence of a vaginal plug was used as an indication of E0 (embryonic day 0). Fetal mice at stage E11.5, E13.5, E14.5, E16.5 and E18.5 were used for immunohistochemistry and stages E13.5 to E18.5 for real time PCR and western blot.

Tissue preparation

Following ether anaesthetisation, pregnant mice were sacrificed by cervical dislocation, and the heads of fetal mice were removed and fixed in 4 % paraformaldehyde in 0.1 M phosphate buffer (pH 7.4) at room temperature for 20 h, then embed in paraffin. Sagittal and frontal Sects. (5 μ m) were cut for haematoxylin and eosin (HE) staining and immunohistochemistry. The first mandibular molar tooth germs were dissected under stereomicroscope.

Antibodies and immunohistochemistry

A SABC kit (Boster, Wuhan, China) was used for immunohistochemistry. The primary antibodies used for immunohistochemistry were as follows: HA (Abcam, ab-53842), HAS1 (Bioss, bs-2946r), HAS2 (Santa Cruz, sc-365263) and HAS3 (Santa Cruz, sc-34204). Secondary antibodies were all purchased from Boster in China (BA-1003, BA-1004, BA-1006). In brief, the slides were deparaffinized and rehydrated by gradient elution using xylene and ethanol, followed by incubation in 3 % H₂O₂ to suppress endogenous peroxidase activity. For antigen retrieval, the slides were incubated in sodium citrate buffer and heated in a microwave oven, followed by cooling at room temperature. A concentration of 5 % BSA was dropped onto the slides for 20 min at room temperature prior to incubation overnight in primary antibody at 4 °C. The sections were incubated with biotinylated secondary antibody. An SABC kit was used for subsequent staining. 3, 3'-Diaminobenzidine (DAB) or 3-Amino-9-ethyl carbazol (AEC) was used as color developing agents; then, the slides were counterstained with hematoxylin. Finally, slides were mounted with Permount TM Mounting Medium, and observed on a microscope (Nikon Eclipse 80i, Japan).

RNA extraction and real-time PCR analysis

Total RNA was extracted from tooth germs using TRIzol (Invitrogen). Approximately 1 μ g total RNA was used to synthesize cDNA with the RevertAid First strand cDNA Synthesis Kit (Thermo Scientific). HAS1, HAS2, HAS3 expression levels were evaluated. Glyceraldehyde-3-phosphate dehydrogenase (GAPDH) was used as a control to normalize RNA expression levels. Real-time polymerase chain reaction (PCR) was performed with an ABI 7500

real-time PCR system (Applied Biosystem, Foster City, CA) and the SYBR green SuperReal PreMix Plus (FP205, Tiangen, China). A Ct value was obtained for each sample, the fold-change in gene expression relative to the control was calculated by the $2^{-\Delta\Delta Ct}$ method. Primer sequences used in Real-Time PCR are listed in Table 1.

Western blot

The primary antibodies and secondary antibodies used against HAS1, HAS2 and HAS3 for western blot were the same as those used for immunohistochemistry. An antibody against β -actin was used as an internal reference (Abcam, ab-129348). Total protein was extracted using RIPA Lysis Buffer (50 mmol/L TrisHCl, pH 7.4, 150 mmol/L NaCl, 1 % NP40, 0.25 % Na-deoxycholate, 1 mmol/L phenylmethanesulfonyl fluoride) containing phenylmethanesulfonyl fluoride (Beyotime, Haimen, China). Equivalent amounts of diluted protein samples were separated through 6–10 % Trisglycine sodium dodecylsulfate–polyacrylamide gel electrophoresis (Novex, San Diego, CA). The proteins were subsequently transferred onto a polyvinylidene fluoride membrane and blocked for 2 h at room temperature in 5 % skim milk solution, followed by incubation in primary antibody overnight at 4 °C. After the membranes were washed, secondary antibodies were incubated for 1 h at room temperature. Finally, protein bands were visualized with Super Signal (Thermo Scientific) chemiluminescence horseradish peroxidase substrate according to the manufacturer’s instructions and analyzed with an Image Quant LAS4000 (GE Healthcare Life Sciences, Piscataway, NJ).

Statistical analysis

Data were analyzed using SPSS (Statistical Package for Social Science, Chicago, IL, USA) version 20.0. Mean values were calculated and are presented, and error bars represent \pm SD. A two-tailed *t* test was used for the two-subgroup comparisons. Statistical significance was accepted at $p < 0.05$ for all analyses.

Results

HA and HAS immunostaining in embryonic mouse molars

The first mandible mouse tooth germ was at the initial stage at E11.5 (Fig. 1a). HA was weakly detected in the thickened dental epithelium (Fig. 1f). We also weakly detected the three HASs in the dental epithelium in a similar pattern (Fig. 2a, e, i). We did not detect any HA or HAS immunostaining in the basement membrane or its underlying dental mesenchyme (Figs. 1f, 2a, e, i).

At E13.5, the tooth germ was shaped like a bud (Fig. 1b). HA was expressed in the central regions of the tooth bud and weakly stained the adjacent condensed dental mesenchyme (Fig. 1g). We also detected all three HASs in the center of the tooth bud, but HAS1 immunostaining was stronger than the other two HASs. HAS3 was clearly expressed in the underlying condensed dental mesenchyme, while HAS1 and HAS2 were not (Fig. 2b, f, j). Interestingly, antibodies against HA and HAS3 intensely stained the jaw mesenchyme surrounding the tooth bud and the condensed dental mesenchyme (Figs. 1g, 2j).

The tooth germ was at the cap stage at E14.5 (Fig. 1c). HA immunostaining was intense in the stellate reticulum and the dental follicle and moderately positive in the dental papilla and weakly positive in the inner and outer enamel epithelium (IEE and OEE) (Fig. 1h). All three HASs were strongly stained in the stellate reticulum. HAS1 and HAS2 moderately stained the IEE and OEE, while HAS3 intensely stained the IEE adjacent to the primary enamel knot. In addition, all three HASs were expressed in the dental papilla, and HAS3 was most strongly detected (Fig. 2c, g, k).

At E16.5, the enamel organ resembled a bell (Fig. 1d). HA immunostaining expression was stronger in the stellate reticulum (SR), stratum intermedium (SI) and the dental papilla compared to E14.5. HA immunostaining was weak in the OEE and IEE, as well as in the dental mesenchyme adjacent to the IEE (Fig. 1i). The expression patterns of HAS1 and HAS3 were identical to HA (Fig. 2d, l). HAS2 was moderately detected in the stellate reticulum and the

Table 1 Primers sequences used in the real time PCR

Gene	Forward primer	Reverse primer	bp
HAS-1	TCACCATCTCAGCCTACCAAG	AGTTGCCATCCCACACATAAG	201
HAS-2	GCAATCTGTGAAAAGGCTGAC	ATTTGTCCCTGCCATAACTT	119
HAS-3	TGGGTCTACATCTGCTCATCC	GTATTCGGGGTCTCTTGGA	149
GAPDH	GACATCAAGAAGGTGGTGAAGC	GAAGGTGGAAGAGTGGGAGTT	117

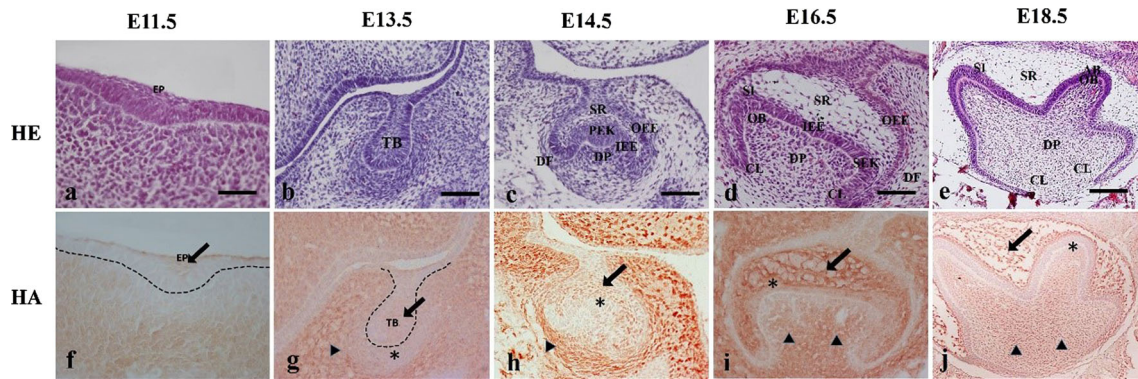


Fig. 1 Immunohistochemical staining for HA in the first mandibular embryonic tooth germs. **a–e** HE staining for tooth germ at E11.5, E13.5, E14.5, E16.5 and E18.5. **f** HA immunostaining was weakly positive in the dental epithelium (*arrow* in **f**). **g** HA was expressed in the central tooth bud (*arrow* in **g**), and weakly expressed in the underlying condensed dental mesenchyme (* in **g**), and strongly expressed in the jaw mesenchyme surrounding the condensed mesenchyme (*arrowhead* in **g**). **h** HA expression was detected in the stellate reticulum (*arrow* in **h**), moderately detected in the dental papilla, and strongly detected in the dental follicle (*arrow* in **h**). The

staining in the stratum intermedium (* in **h**). **i** HA staining in the stellate reticulum (*arrow* in **i**), stratum intermedium (* in **i**) and dental papilla (*arrowhead* in **i**). **j** HA was strongly detected in the stellate reticulum and the dental papilla (*arrow* in **j**) and was not expressed in the ameloblast, odontoblast (* in **j**). *TB* tooth bud; *AB* ameloblast; *OB* odontoblast; *CL* cervical loop; *DP* dental papilla; *DF* dental follicle; *SR* stellate reticulum; *SI* stratum intermedium; *OEE* outer enamel epithelium; *IEE* inner enamel epithelium; *PEK* primary enamel knot; *SEK* secondary enamel knot. Scale bar = 100 μ m (**a**, **b**, **c**). Scale bar = 50 μ m (**d**, **e**)

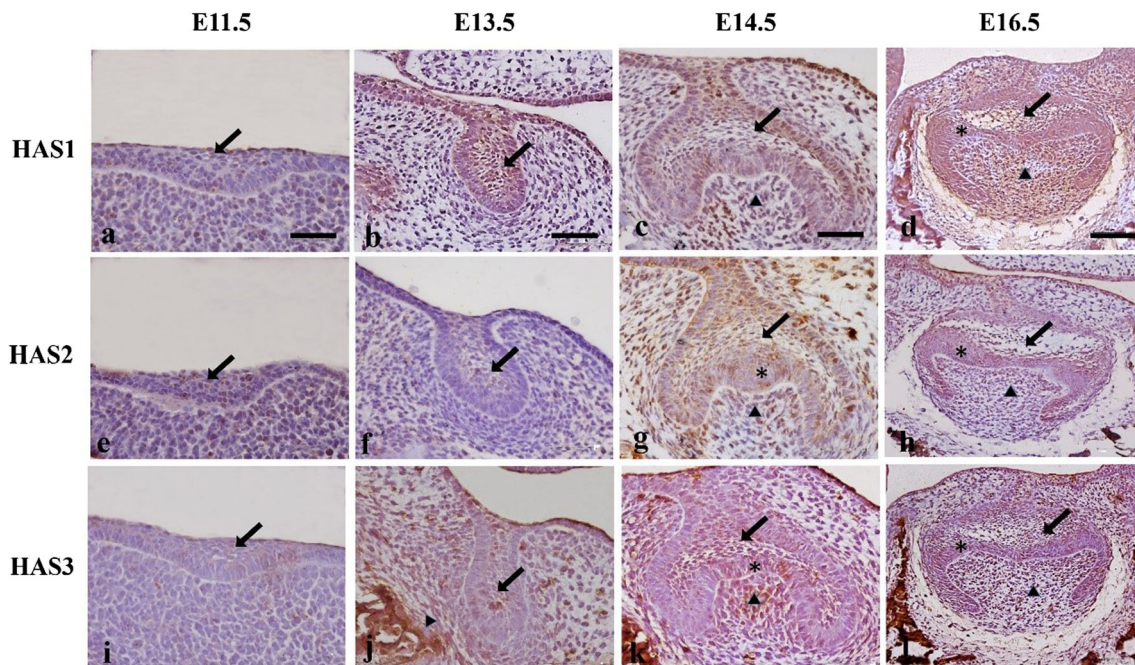


Fig. 2 HE and immunohistochemistry for HAS1, HAS2 and HAS3. **a**, **e**, **i** HAS1, 2, 3 expression was detected in the dental epithelium at E11.5 (*arrow* in **a**, **e**, **i**). **b**, **f**, **j** At E13.5, HAS1, 2, 3 were detected in the tooth bud and the dental epithelium (*arrow* in **b**, **f**, **j**), and HAS3 also intensely stained the underlying condensed dental mesenchyme (*arrowhead* in **j**). **c**, **g**, **k** HASs were expressed in the stellate reticulum, inner and outer enamel epithelium (*arrow* in **c**, **g**, **k**), and

the dental papilla (*arrowhead* in **c**, **g**, **k**) and was also detected in the PEK (* in **c**, **g**, **k**). **d**, **h**, **l** HAS1, 2, 3 were all detected in the stellate reticulum (*arrow* in **d**, **h**, **l**) and SEK (* in **d**, **h**, **l**). In the dental papilla, HAS1 and HAS3 were expressed (*arrowhead* in **d**, **l**), while HAS2 was moderately expressed in the dental papilla underlying the basement membrane (*arrowhead* in **h**). Scale bar = 100 μ m (**a**, **b**). Scale bar = 50 μ m (**c**, **d**)

dental papilla underlying the basement membrane, while it was strongly expressed in the IEE and OEE (Fig. 2h).

At E18.5, the odontoblast and the ameloblast had begun to undergo cytodifferentiation (Fig. 1e). HA

localization in the stellate reticulum, stratum intermedium and the dental papilla was similar to that at E16.5. Interestingly, HA was also expressed in the preameloblast and preodontoblast, but immunostaining in the mature

ameloblast and odontoblast disappeared. In particular, HA expression in the dental papilla gradually increased from the crown to the cervical loop (Fig. 1j). The expression pattern of the three HASs in the enamel organ and the region of the odontoblast, ameloblast was similar to that of HA (Fig. 3a, d, g). HAS1 was expressed in the dental papilla (Fig. 3a, b), while HAS2 and HAS3 were primarily expressed in the subodontoblastic layer of the coronal pulp (Fig. 3d, e, g, h). HAS1 and HAS2 were strongly expressed in the cervical loop regions, while HAS3 was weakly expressed (Fig. 3c, f, i).

Changes in HAS mRNA levels during mouse molar development

HAS1 and HAS2 mRNA expression both decreased, while HAS3 increased from the cap stage (E14.5) to the late bell stage (E18.5) (Fig. 4a–c). HAS2 and HAS3 mRNA expression was significantly different at all the stages examined. HAS1 mRNA levels were significantly different between E14.5 and E16.5, but not between E16.5 and E18.5 or between E14.5 and E16.5 (Fig. 4a). These experiments were performed in triplicate.

Western blot results

By using β -actin as an internal reference, we found similar changes in HAS protein levels as those observed for mRNA levels. HAS1 protein levels were similar at E13.5 and E14.5, while it dramatically decreased at E16.5 and E18.5. HAS2 expression was similar to HAS1, but its expression level was lower at E14.5 than at E13.5. Interestingly, HAS3 was highly expressed at E16.5 and E18.5, but almost undetectable at E13.5 and E14.5 (Fig. 4d). Western blotting was repeated three times.

Discussion

We performed this study to compare the localization and expression of HA and HASs in the first embryonic mouse molars at various stages. We found that HA and its synthases were expressed in a temporal-spatial pattern, and the expression level of the three HASs dramatically changes among the different stages.

It is well known that tooth morphogenesis requires the interaction between the dental epithelium and dental mesenchyme (Mitsiadis and Graf 2009). In mice, the first

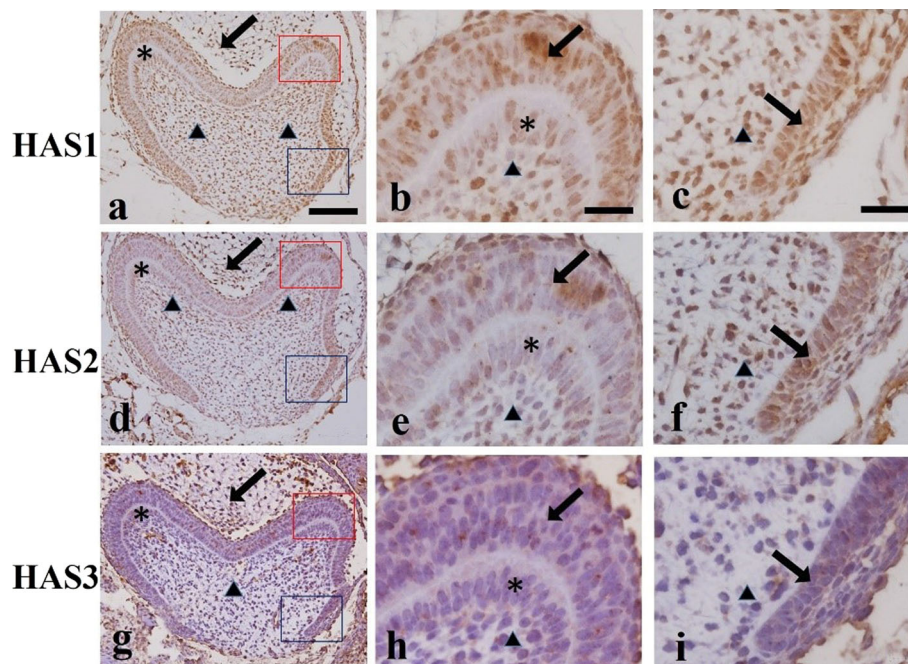
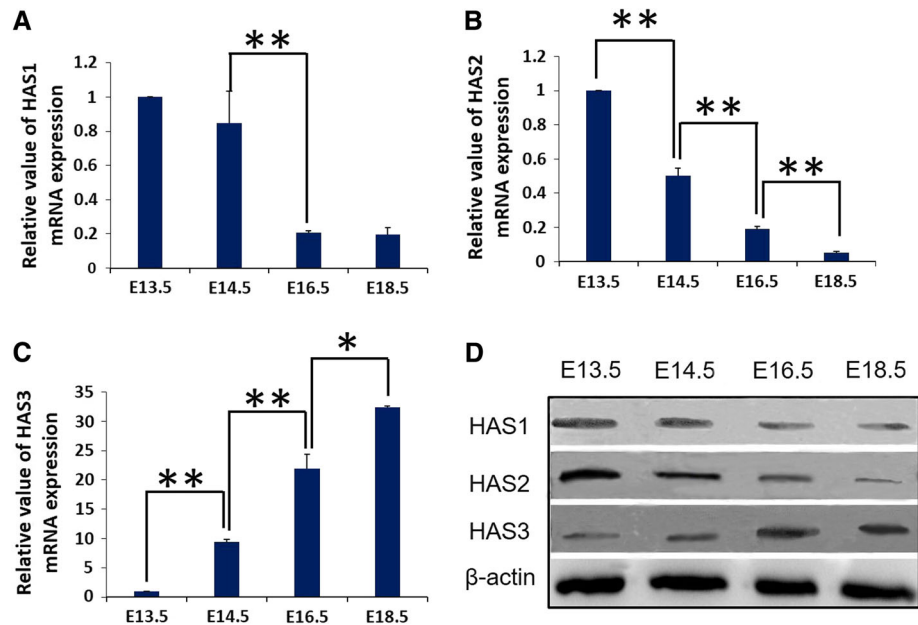


Fig. 3 Immunohistochemistry staining for HAS1, HAS2 and HAS3 at E18.5. The red box in a, d, g corresponds to (b), (e), (f), while the blue box in (a), (d), (g) corresponds to (c), (f), (i), respectively. (a, d, g) HAS1, 2, 3 was detected in the ameloblast, odontoblast (* in a, d, g), dental papilla (arrowhead in a, d, g) and stellate reticulum (arrow in a, d, g). (b, e, h) HASs were all expressed in the ameloblast (arrow

in b, e, h), odontoblast (* in b, e, h) and subodontoblastic layer of the coronal pulp (arrowhead in b, e, h). The HASs were all be stained positively. (c, f, i) Three HASs were all detected in the dental papilla (arrowhead in c, f, i), and the cervical loop, HAS1 and HAS2 were strongly expressed (arrow in c, f, i). Scale bar = 100 μ m (a). Scale bar = 25 μ m (b, c)

Fig. 4 Real time PCR and western blot analysis for HAS1, HAS2 and HAS3 during tooth germ development. Changes in mRNA levels of HAS1 (a), HAS2 (b), HAS3 (c) at E13.5, E14.5, E16.5 and E18.5. Changes in HAS proteins (d) at E13.5, E14.5, E16.5 and E18.5 were revealed by western blot. Data are shown as the mean \pm SD; $n = 3$. * $p < 0.05$, ** $p < 0.01$ (Student's *t* test)



morphological sign of tooth development appears as a local thickening of the dental epithelium. At E11.5, HA and all three HASs were expressed in the dental epithelium cells, but not in the basement membrane or its adjacent dental mesenchyme. This was not completely consistent with a previous study that showed that HAS1 expression was lost after E8.5 (Tien and Spicer 2005). However, we clearly detected HAS1 protein at E11.5, and detected HAS1 mRNA and protein at later stages. A previous study demonstrated that the extracellular and pericellular matrix surrounding the migrating and proliferating cells highly expressed HA during embryogenesis. During the initial stages of tooth development, the dental epithelium is highly proliferative. Therefore, HA and HASs may play a significant role in tooth germ initiation.

When the thickened dental epithelium proliferated and invaginated into the subjacent mesenchyme to form the epithelial tooth bud at E13.5, we detected HA and all three HASs in the center of the epithelial bud. Previous studies demonstrated that the function of HA was dependent on its molecular weight. It was found that HAS1 and HAS2 synthesized HMW HA was, while HAS3 synthesized LMW HA. HMW HA facilitates cell contact inhibition and cell migration, while LMW HA enhances ECM remodeling (Monslow et al. 2015). HAS1 and HAS2, but not HAS3, were highly expressed in the bud stage, which may highlight an important role for HMW HA in cell migration and proliferation during early epithelial morphology. In addition, HA was only weakly detected in the underlying condensed dental mesenchyme, which was consistent with a study that showed that hyaluronan expression decreased in the limb bud periphery where cells aggregated (Knudson

2003). Conversely, the weak staining of HAS1 and HAS2 in condensed regions supports their roles in cell contact inhibition, and the strong HAS3 staining may suggest its role in the connection of the condensed cells. Interestingly, HA and HAS3 were also intensely expressed in the jaw mesenchyme, which surrounded the tooth bud and condensed mesenchyme. The results suggest that the function of HA was distinct in the tooth germ and the jaw mesenchyme, and the abundant HA in the jaw mesenchyme provided enough space for the dental epithelium to invaginate into the mesenchyme.

From the cap to the bell stage, enamel organ morphogenesis occurred, and reciprocity between the cells in different layers and their derivatives is necessary (Weigel et al. 1997; Thesleff 2000). It has been previously demonstrated that this involves cell proliferation, differentiation, adhesion and migration and that HA contributes to each function (Toole 2001). HA and HAS were expressed in the stellate reticulum. This finding suggests that as a hydrophilic component (Monslow et al. 2015), HA increased the volume of the enamel organ extracellular compartment and detached the central cells, which is essential for nutrient exchange and protection of enamel organs development (Ida-Yonemochi et al. 2005). Moreover, its binding proteins, including versican (Jiang et al. 2010) and its primary receptor CD44 (Felszeghy et al. 2001), were also expressed in the SR, which further emphasizes their interactions for enamel organ formation. We also detected HA and HAS in the stellate reticulum at a similar intensity as the stratum intermedium. In addition to regulating the IEE cell phenotype, the SI also contributed to ameloblasts development (Lesot et al. 2014). It has been

suggested that SI cells required changes to their plasma membrane composition (Nakamura and Ozawa 1997) where HA localized, and thus perhaps participated in regulating amelogenesis for enamel organ formation. Overall, HA has been shown to participate in the nutritional recruitment from the outer layer and enamel organ enlargement, but its specific role in cell proliferation, differentiation and migration requires more detailed investigation. In addition, HAS1 and HAS2 expression significantly decreased, and HAS3 expression significantly increased, suggesting that they have different functions in enamel organ morphogenesis. In addition, the shape and size of the tooth crown are determined by epithelial growth and folding, and the progress is regulated by the enamel knot, which has been demonstrated to be a signaling center (Thesleff et al. 2001; Lesot and Brook 2009). The strong HAS2 and HAS3 staining at the enamel knot suggests that they play a significant role in the signaling regulation of enamel formation. Although the localization of HA and HASs was not obviously different in this region, the significant increase in HAS3 expression, and its distinctive localization in the enamel knot adjacent to the IEE suggest that it may have a specific function there in regulating enamel formation.

The crown form was established during the late bell stage (Thesleff and Jernvall 1997), and terminal differentiation occurs in the cells of the inner enamel epithelium and the peripheral cell layer in the dental papilla (Lesot et al. 1981). The IEE becomes the enamel-producing ameloblasts, and the periphery of the dental papilla will differentiate into the dentin-producing odontoblasts (Tompkins 2006). In the current study, we detected HA in the preameloblast and preodontoblast, but did not detect HA expression in the mature ameloblast or odontoblast upon differentiation. These results were consistent with previous studies Felszeghy et al. (2000). These results may imply that HA plays a transitory role in the early phase of presecretory ameloblasts and odontoblasts proliferation, enamel development and dentin matrix organization. The strong HA staining biosynthesized by HAS1 and HAS2 but not HAS3 in the IEE were proposed to play a role for the ameloblasts. In addition, HAS expression gradually decreased in the odontoblasts and ameloblasts (Felszeghy et al. 2005), which may suggest that hyaluronan is separately synthesized by each HAS isoforms to contribute to the regulation of early dentin and enamel formation. Furthermore, HA expression in the dental papilla gradually increased from the crown to the root, with strong expression in the cervical loop, which was essential for root formation (Chen et al. 2014; Wang et al. 2014). All of these results suggest that HA and HAS functions in the development of dental pulp and the future root.

In conclusion, HA is expressed in a temporal-spatial expression pattern and may play a role in embryonic tooth morphogenesis. The difference in the distribution and expression of the three HASs at different developmental stages also supports their roles in cell proliferation, cell differentiation and cell migration. The exact mechanism by which the three HAS isoforms influence the tooth germ development is still unknown. Therefore, it will be important to determine the function of each HAS alone and to determine how HA interacts with other binding proteins and receptors.

Acknowledgments This work was supported by National Natural Science Foundation of China (Nos. 81570965 and 81170951) and the Shanghai Science and Technology Commission Program (Nos. 124119A7400 and 15411965800).

Compliance with ethical standards

Conflicts of interests None.

References

- Bei M (2009) Molecular genetics of tooth development. *Curr Opin Genet Dev* 19(5):504–510
- Camenisch TD, Spicer AP, BrehmGibson T et al (2000) Disruption of hyaluronan synthase2 abrogates normal cardiac morphogenesis and hyaluronan-mediated transformation of epithelium to mesenchyme. *J Clin Invest* 106(3):349–360
- Chen X, Chen G, Feng L et al (2014) Expression of Nfic during root formation in first mandibular molar of rat. *J Mol Histol* 45(6):619–626
- Evanko SP, Tammi MI, Tammi RH et al (2007) Hyaluronan-dependent pericellular matrix. *Adv Drug Deliv Rev* 59(13):1351–1365
- Felszeghy S, Hyttinen M, Tammi R et al (2000) Quantitative image analysis of hyaluronan expression in human tooth germs. *Eur J Oral Sci* 108(4):320–326
- Felszeghy S, Módis L, Tammi M et al (2001) The distribution pattern of the hyaluronan receptor CD44 during human tooth development. *Arch Oral Biol* 46(10):939–945
- Felszeghy S, Mészár Z, Prehm P et al (2005) The expression pattern of hyaluronan synthase during human tooth development. *Arch Oral Biol* 50(2):175–179
- Ida-Yonemochi H, Ohshiro K, Swelam W et al (2005) Perlecan, a basement membrane-type heparan sulfate proteoglycan, in the enamel organ: its intraepithelial localization in the stellate reticulum. *J Histochem Cytochem* 53(6):763–772
- Itano N (2008) Simple primary structure, complex turnover regulation and multiple roles of hyaluronan. *J Biochem* 144(2):131–137
- Itano N, Kimata K (2002) Mammalian hyaluronan synthases. *IUBMB Life* 54(4):195–199
- Jiang BZ, Yokohama-Tamaki T, Wang ZL et al (2010) Expression, localisation and synthesis of versican by the enamel organ of developing mouse molar tooth germ: an in vivo and in vitro study. *Arch Oral Biol* 55(12):995–1006
- Jiang D, Liang J, Noble PW (2011) Hyaluronan as an immune regulator in human diseases. *Physiol Rev* 91(1):221–264
- Knudson CB (2003) Hyaluronan and CD44: strategic players for cell-matrix interactions during chondrogenesis and matrix assembly. *Birth Defects Res C Embryo Today* 69(2):174–196

- Lei H, Liu H, Ding Y et al (2014) Immunohistochemical localization of Pax6 in the developing tooth germ of mice. *J Mol Histol* 45(4):373–379
- Lesot H, Brook AH (2009) Epithelial histogenesis during tooth development. *Arch Oral Biol* 54(Suppl 1):S25–S33
- Lesot H, Osman M, Ruch JV (1981) Immunofluorescent localization of collagens, fibronectin, and laminin during terminal differentiation of odontoblasts. *Dev Biol* 82(2):371–381
- Lesot H, Hovorakova M, Peterka M et al (2014) Three-dimensional analysis of molar development in the mouse from the cap to bell stage. *Aust Dent J* 59(Suppl 1):81–100
- Mitsiadis TA, Graf D (2009) Cell fate determination during tooth development and regeneration. *Birth Defects Res C Embryo Today* 87(3):199–211
- Monslow J, Govindaraju P, Puré E (2015) Hyaluronan—a functional and structural sweet spot in the tissue microenvironment. *Front Immunol* 6:231
- Nakamura H, Ozawa H (1997) Immunolocalization of CD44 and the ezrin-radixin-moesin (ERM) family in the stratum intermedium and papillary layer of the mouse enamel organ. *J Histochem Cytochem* 45(11):1481–1492
- Shibata S, Kaneko S, Yanagishita M et al (1999) Histochemical localization of hyaluronan and versican in the rat molar dental pulp. *Arch Oral Biol* 44:373–376
- Shibata S, Yoneda S, Yanagishita M et al (2002) Developmental changes and regional differences in histochemical localization of hyaluronan and versican in postnatal molar dental pulp. *Int Endod J* 35:159–165
- Siiskonen H, Oikari S et al (2015) Hyaluronan synthase 1: a mysterious enzyme with unexpected functions. *Front Immunol* 5(6):43
- Stern R, Asari AA, Sugahara KN (2006) Hyaluronan fragments: an information-rich system. *Eur J Cell Biol* 85(8):699–715
- Thesleff I (2000) Genetic basis of tooth development and dental defects. *Acta Odontol Scand* 58:191–194
- Thesleff I (2003) Epithelial-mesenchymal signaling regulating tooth morphogenesis. *J Cell Sci* 116(Pt 9):1647–1648
- Thesleff I, Jernvall J (1997) The enamel knot: a putative signaling center regulating tooth development. *Cold Spring Harb Symp Quant Biol* 62:257–267
- Thesleff I, Keränen S, Jernvall J (2001) Enamel knots as signaling centers linking tooth morphogenesis and odontoblast differentiation. *Adv Dent Res* 15:14–18
- Tian X, Azpurua J, Hine C (2013) High-molecular-mass hyaluronan mediates the cancer resistance of the naked mole rat. *Nature* 499(7458):346–349
- Tien JY, Spicer AP (2005) Three vertebrate hyaluronan synthases are expressed during mouse development in distinct spatial and temporal patterns. *Dev Dyn* 233(1):130–141
- Tompkins K (2006) Molecular mechanisms of cytodifferentiation in mammalian tooth development. *Connect Tissue Res* 47(3):111–118
- Toole BP (2001) Hyaluronan in morphogenesis. *Semin Cell Dev Biol* 12:79–87
- Vigetti D, Karousou E, Viola M et al (2014) Hyaluronan: biosynthesis and signaling. *Biochim Biophys Acta* 1840(8):2452–2459
- Wang Y, Lv L, Yu X et al (2014) The characteristics of epithelial cell rests of Malassez during tooth eruption of development mice. *J Mol Histol* 45(1):1–10
- Wang S, Zhen L, Liu Z et al (2015) Identification and analysis of the promoter region of the human HAS3 gene. *Biochem Biophys Res Commun* 460(4):1008–1014
- Weigel PH, Hascall VC, Tammi M (1997) Hyaluronan synthases. *J Biol Chem* 272:13997–14000
- Xie M, Xing G, Hou L et al (2015) Functional role of EMMPRIN in the formation and mineralisation of dental matrix in mouse molars. *J Mol Histol* 46(1):21–32